Beyond Frame-wise Tracking: A Trajectory-based Paradigm for Efficient Point Cloud Tracking

BaiChen Fan[1†], Sifan Zhou[2†*], Jian Li[1], Shibo Zhao[2], Muqing Cao[2], Qin Wang[1‡]

***Abstract*—LiDAR-based 3D single object tracking (3D SOT) is a critical task in robotics and autonomous systems. Existing methods typically follow frame-wise motion estimation or a sequence-based paradigm. However, the two-frame methods are efficient but lack long-term temporal context, making them vulnerable in sparse or occluded scenes, while sequence-based methods that process multiple point clouds gain robustness at a significant computational cost. To resolve this dilemma, we propose a novel trajectory-based paradigm and its instantiation, TrajTrack. TrajTrack is a lightweight framework that enhances a base two-frame tracker by implicitly learning motion continuity from historical bounding box trajectories alone—without requiring additional, costly point cloud inputs. It first generates a fast, explicit motion proposal and then uses an implicit motion modeling module to predict the future trajectory, which in turn refines and corrects the initial proposal. Extensive experiments on the large-scale NuScenes benchmark show that TrajTrack achieves new state-of-the-art performance, dramatically improving tracking precision by 4.48% over a strong baseline while running at 56 FPS. Besides, we also demonstrate the strong generalizability of TrajTrack across different base trackers. Code and video will be available.**

I. INTRODUCTION

3D single object tracking (3D SOT) is a fundamental task in computer vision with wide applications in autonomous driving and robotics. It aims to accurately track a target across frames using LiDAR or cameras. Compared to camera images, LiDAR point clouds offer notable advantages: robust to light changes and capture rich geometric semantics from environments. These strengths make it well-suited for robust perception in robotics. However, challenges from point cloud inherent sparsity, especially under occlusion, and appearance changes due to motion or blur often lead to incomplete observations, making reliable tracking difficult.

Previous methods typically follow a two-frame paradigm (Fig.1(a)), which can be categorized into appearance-based [1]–[8] and motion-based approaches [9]–[15]. Similarity-based methods such as SC3D [1], P2B [3], and PTT [6] rely on frame-wise appearance cues between template and search point cloud and perform similarity matching, but they are sensitive to appearance changes and fast motion. In contrast, motion-based methods like M^2-Track series [9], [10] and P2P [16] explicitly model inter-frame motion to estimate relative translation. However, by relying solely on two-frame information, they all struggle in sparse or occluded scenes due to limited appearance or motion clues. More critically, they lack considerations of long-term motion continuity, preventing them from forming a predictive motion prior—for example, anticipating a vehicle's position as it moves through a temporary occlusion—which is essential for robust tracking.

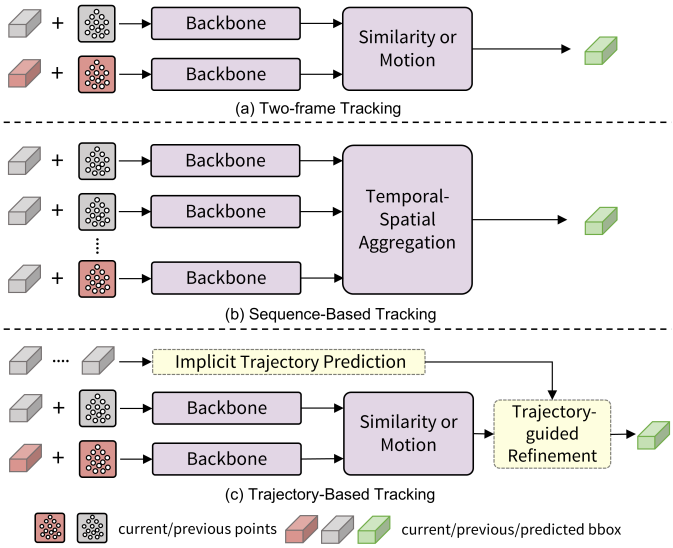

Fig. 1: Different tracking paradigms. (a) Two-frame paradigm exploits two-frame inputs for tracking through appearance matching or motion prediction. (b) Sequence-based paradigm uses multi-frames inputs to integrate target information. (c) Our Trajectory-based paradigm considers both short- and long-term motion clues.

To overcome these challenges, recent studies have explored the sequence-based paradigm (Fig.1(b)), which incorporates long-term temporal information by processing multiple point cloud frames. For instance, STTracker [17] processes a sequence of BEV feature maps and uses a deformable attention mechanism to aggregate spatio-temporal features. Going a step further, SeqTrack3D [18] utilizes sequences of both point clouds and their corresponding historical bounding boxes, using a Seq2Seq model to explicitly learn motion patterns. While these approaches improve robustness in sparse scenes, they introduce a critical trade-off. Their reliance on processing multi-frame point clouds inevitably leads to a high computational cost, making them less suitable for latency-sensitive, real-time tracking applications. Besides, their complex feature extraction from sequential data can still struggle to learn a clear, consistent motion trajectory, especially with noisy or occluded frames. This leaves a clear opening for a method that can leverage long-term motion continuity in a more lightweight and direct manner.

In this paper, we propose **TrajTrack**, a novel 3D

This work is supported by the Industrial Prospect and Key Core Technology Projects of Jiangsu provincial key R & D Program (Grant No. BE2022071) and the Innovation Program for Quantum Science and Technology (2024ZD0300900).

†Equal Contribution. *Project Leader. ‡Corresponding Author.

[1]BaiChen Fan, Jian Li, and Qin Wang are with the Institute of Quantum Information and Technology, Nanjing University of Posts and Telecommunications, Nanjing, China.

[2]Sifan Zhou, Shibo Zhao and Muqing Cao are with the Robotics Institute, Carnegie Mellon University, PA, USA.

SOT framework (Fig.1(c)), that synergistically combines the strengths of short-term explicit motion and long-term implicit continuity through a two-stage process. **Stage 1: Explicit Motion Proposal:** We first employ an efficient, two-frame explicit motion model. By analyzing two inter-frame point clouds, this stage rapidly generates an initial tracking proposal. This proposal effectively captures instantaneous motion but can be prone to errors in sparse or occluded scenes. **Stage 2: Implicit Trajectory Prediction:** This is the core innovation of our framework. We introduce an implicit motion modeling module that operates solely on the historical sequence of bounding box. It uses a lightweight Transformer to learn the object's long-term motion continuity and predict future trajectory with confidence. **Post-process: Trajectory-guided Proposal Refinement:** Finally, we design a proposal refinement mechanism. It leverages the predicted trajectory from Stage 2, which embodies a long-term motion prior, to intelligently calibrate and correct the potentially inaccurate initial proposal from Stage 1. By integrating short-term explicit observations with long-term, consistent motion patterns, TrajTrack effectively captures both local and global motion cues. Its key innovation lies in enhancing tracking robustness by exploiting the intrinsic continuity of object motion, without the high computational cost of processing multiple point cloud frames. Extensive experiments demonstrate the superior performance and real-time speed of our approach. In summary, our main contributions are as follows:

- **Trajectory-based Paradigm**: We propose a novel trajectory-based paradigm that leverages historical bboxes to incorporate long-term motion continuity, enhancing robustness without the overhead of multi-frame input.
- **TrajTrack with Implicit Motion Modeling**: We instantiate this paradigm in TrajTrack, a framework featuring a novel Implicit Motion Modeling (IMM) module to provide predictive priors to synergize long-term continuity with short-term observations.
- **SOTA Performance**: We achieve new state-of-the-art performance on the large-scale nuScenes benchmark by a significant margin (+4.48% in Precision). Besides, we demonstrate the strong generalizability by consistently improving the existing method's performance.

II. Related Work

Single Object Tracking on Point Clouds. The field of SOT has evolved significantly, driven by advancements in point cloud processing [19]–[24] and the image domain [25]–[27]. The pioneering work SC3D [1] applied Siamese networks directly to point clouds, and introduced template matching, but suffered from inefficiency and non-end-to-end training. Addressing these limitations, P2B [3] leveraged a Region Proposal Network (RPN) and VoteNet [28] for real-time proposal generation. 3D-SiamRPN [4] also has a similar pipeline. Follow-up methods like BAT [5] fused box-aware structural features, PTT [6], [7] introduced the transformer, and V2B [29] transformed sparse points into dense bird's-eye-view maps. Attention mechanisms were also integrated by STNet [30], LTTR [31], and PTTR [8], to propagate target-specific features. Despite progress, appearance-based methods struggled with inefficient geometry in sparse or occlusion scenes. This prompted motion-centric paradigms: M^2-Track [9] modeled inter-frame target motion by a "segmentation and tracking" pipeline. Furthermore, M²Track++ [10] extended the paradigm to semi-supervised applications. To incorporate historical data, DMT [11] predicts the target's center from past bounding boxes. Recently, P2P [16] considered the context relationship between the background; it inferred the relative motion directly from the cropped point clouds of two consecutive frames. However, these approaches focused on short-term temporal inputs, overlooking long-term historical frames. Recently, TAT [32] addressed this by aggregating historical templates via RNNs but failed to handle low-quality templates. STTracker [17] uses a deformable attention mechanism to aggregate spatio-temporal features from a sequence of BEV feature maps. SeqTrack3D [18] proposed a Sequence-to-Sequence paradigm, considered temporal clues of the target in points and box sequences, and extracted both key geometry and motion information from the point clouds sequence. While recent sequence-based methods improve robustness, they struggle to achieve a better trade-off between accuracy and efficiency due to the high overhead of multi-frame processing and the difficulty of learning consistent motion from complex sequential data.

Sequence Modeling for Motion. Learning motion patterns from temporal sequences is a powerful way to incorporate long-term context. In the broader field of trajectory prediction, VectorNet [33] and LaneRCNN [34] pioneered vectorized/rasterized scene representations with graph neural networks (GNNs) to encode dynamic interactions, enabling an end-to-end manner. GATraj [35] further enhanced interaction modeling through graph attention mechanisms. The TNT [36] and DenseTNT [37] frameworks decomposed prediction into hierarchical target selection and dense trajectory generation, significantly improving long-term rationality. In addition, generative models were used to perform trajectory prediction. For instance, variational autoencoders [38], conditional variational autoencoders (CVAEs) [39], and generative adversarial networks (GANs) [40]. Most of these methods follow a seq2seq structure and predict future trajectories using intermediate features of past trajectories. More recently, Transformer-based architectures have become the dominant approach due to their superior ability to model complex, long-range dependencies in sequential data. For instance, S2TNet [41] demonstrated the power of Transformers for spatio-temporal interactions, while AgentFormer [42] introduced agent-centric attention to effectively model the coherence of an individual's trajectory over time. CASPFormer [43] integrated causal spatial priors for socially compliant predictions. The proven success of these models in learning rich patterns from sparse positional sequences directly informs our approach. We are inspired from this powerful sequence modeling paradigm for the specific task of 3D SOT, designing a lightweight IMM module to learn motion continuity from an object's past trajectory.

III. Method

A. Preliminaries

3D Single Object Tracking. In the 3D SOT task, given a sequence of point clouds $\mathbf{P}_t \in \mathbb{R}^{N\times 3}$ at time t with N points

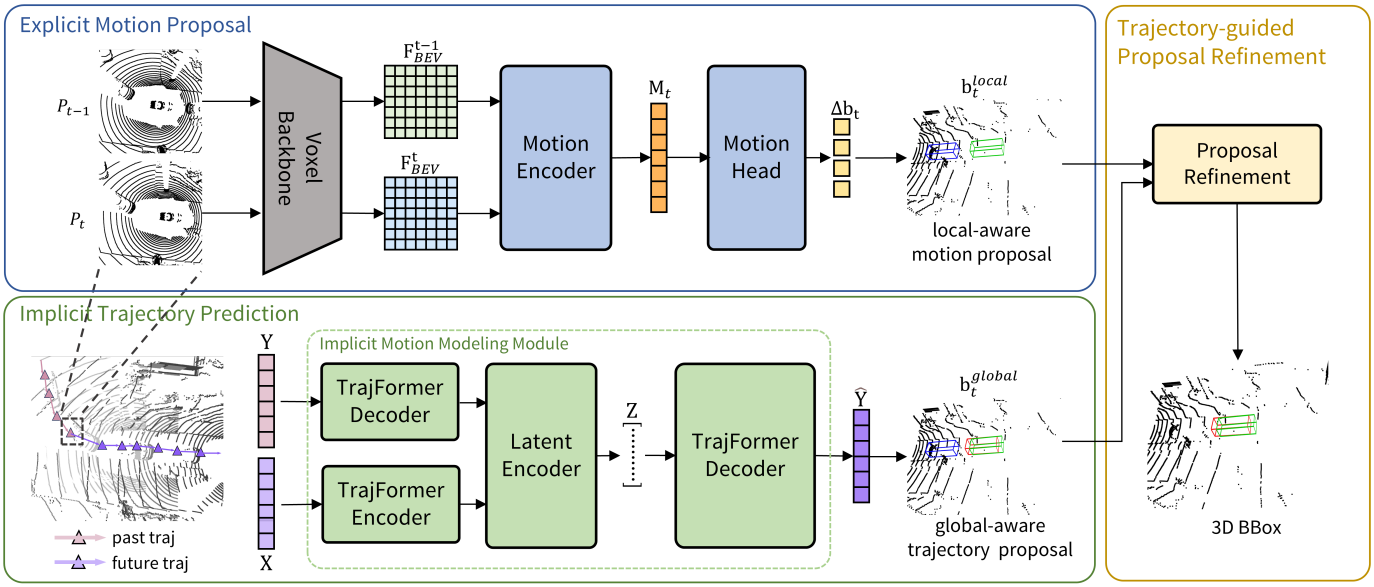

Fig. 2: Overview of proposal Trajectory-based Paradigm and instantiate **TrajTrack**. Explicit Motion Proposal uses a two-frame tracking baseline to obtain the local-aware motion proposal. Implicit Trajectory Prediction is used to learn the object's global-aware motion continuity for trajectory proposal. Finally, Trajectory-guided Proposal Refinement cooperates the local and global-aware motion cues to get the refined 3D BBOX as the final output.

and the initial 3D bounding box $\mathbf{b}_t = (x_t, y_t, z_t, h_t, w_t, l_t, \theta_t) \in \mathbb{R}^{1\times 7}$ in the initial frame t, where (x, y, z) and (h, w, l) represent the center coordinate and size and θ represent the rotation angle. The goal of 3D SOT aims to predict the box $\mathbf{b}_s = (x_s, y_s, z_s, h_s, w_s, l_s, \theta_s) \in \mathbb{R}^{1\times 7}$ in subsequent frames from the search area point cloud. Generally, the object size (h, w, l) will not change in all frames; therefore, the position parameters $(x_s, y_s, z_s, \theta_s)$ need to be predicted.

B. Framework Overview

Our **TrajTrack** framework is designed to address the challenges of 3D SOT by synergistically combining short-term and long-term motion cues. As illustrated in Fig. 2, it follows a two-stage "propose-predict-refine" pipeline: **(1) Explicit Motion Proposal:** First, a two-frame-based explicit motion model rapidly generates an initial, locally-aware tracking proposal for the current frame. **(2) Implicit Trajectory Prediction:** Second, our novel Implicit Motion Modeling (IMM) module learns the object's long-term motion continuity by leveraging only the historical bbox prediction, predicting a globally-aware future trajectory. **(3) Trajectory-Guided Proposal Refinement:** Finally, a post-processing operation from the refinement mechanism uses the trajectory prior to intelligently correct the initial proposal, outputting a more robust tracking result.

C. Stage 1: Explicit Motion Proposal

This stage aims to rapidly generate a high-quality initial proposal that captures instantaneous motion. Recent works [13], [16] have demonstrated the superiority of voxels as a 3D representation in single object tracking (SOT). Therefore, we employ an efficient, voxel-based backbone from [16] to extract BEV features $\mathbf{F}_{t-1}, \mathbf{F}_t \in \mathbb{R}^{H\times W}$ from consecutive point clouds $\mathbf{P}_{t-1}$ and $\mathbf{P}_t$. Notably, we can also use other 3D Tracker [3], [9] in this stage; we also provide the details in Tab. III. These feature maps are concatenated and passed through a motion encoder and a motion head to predict the inter-frame relative motion $\Delta\mathbf{b}_t$:

$$\mathbf{M}t = \mathrm{ME}([\mathbf{F}^{t-1}BEV, \mathbf{F}^{t}_{BEV}]) \quad (1)$$

$$\Delta\mathbf{b}_t = \mathrm{MH}(\mathbf{M}t) \quad (2)$$

where ME and MH are motion encoder and motion head, respectively. Finally, the initial motion proposal $\mathbf{b}_t^{\text{local}}$ for the current frame is obtained by applying this displacement to the previous frame's bounding box $\mathbf{b}t-1$:

$$\mathbf{b}_t^{\text{local}} = \mathbf{b}_{t-1} + \Delta\mathbf{b}_t \quad (3)$$

This local-aware proposal effectively captures local motion but can be prone to errors in sparse or occluded scenes. More details about the Motion Encoder and head can refer to [16].

D. Stage 2: Implicit Trajectory Prediction

The core of our framework is the Implicit Motion Modeling (IMM) module, which learns long-term motion continuity to predict a robust future trajectory. Critically, this module operates solely on the lightweight historical sequence of past bounding box coordinates, $\mathbf{X} = (x^{-H+1}, x^{-H+2}, \ldots, x^0)$, avoiding the high cost of processing multiple point clouds. The IMM module is trained to predict the future trajectory $\mathbf{Y} = (y^0, y^1, \ldots, y^T)$ conditioned on the past trajectory $\mathbf{X}$ and a latent variable $\mathbf{Z}$ that captures the inherent stochasticity of motion. H and T denote historical/future timesteps, respectively. We utilize the input information to predict a set of future trajectories $\hat{\mathbf{Y}}$, from which the trajectory position at the corresponding time step is selected as the global-aware trajectory proposal $\mathbf{b}_t^{global}$. The IMM consists of two main components, which are both implemented using our proposed TrajFormer architecture (Fig. 3).

Motion Continuity Learning. This component's goal is to learn a rich, latent representation of the object's motion patterns. We first process the observed past trajectory $\mathbf{X}$ by

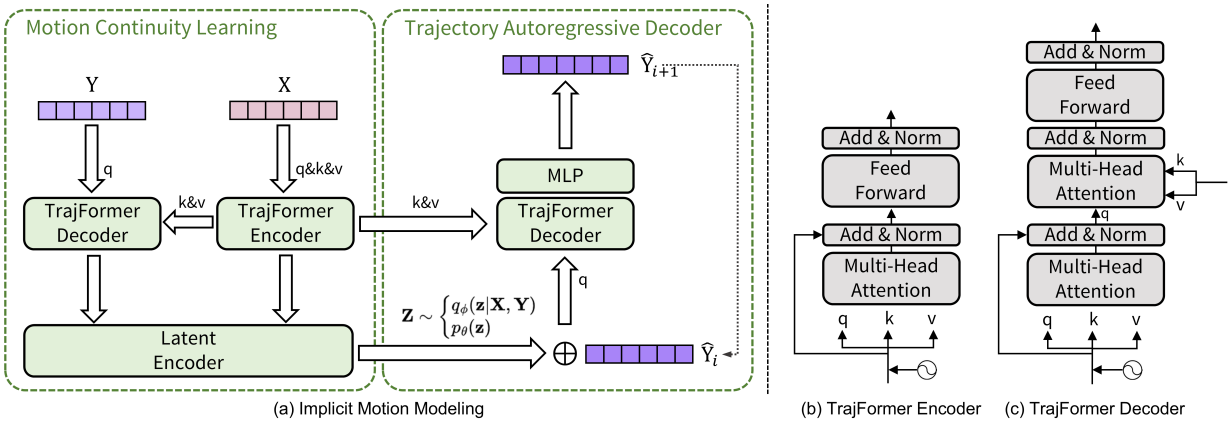

Fig. 3: **(a) Framework of Implicit Trajectory Prediction. (b) The TrajFormer Encoder. (c) The TrajFormer Decoder.**

computing relative displacements $\Delta\mathbf{x}^t = \mathbf{x}^t - \mathbf{x}^{t-1}$ to extract motion-centric features. These features are fed into a TrajFormer Encoder which models the temporal dependencies and outputs parameters for a prior distribution over the latent variable, $p_\theta(\mathbf{Z}|\mathbf{X}) = \mathcal{N}(\mu^p, \mathrm{Diag}(\sigma^p)^2)$.

During training, we additionally leverage the ground-truth future trajectory $\mathbf{Y}$. Its features are fused with the past features and processed by the encoder to parameterize a more informed posterior distribution, $q_\phi(\mathbf{Z}|\mathbf{Y},\mathbf{X}) = \mathcal{N}(\mu^q, \mathrm{Diag}(\sigma^q)^2)$. We enforce consistency between these two distributions by minimizing their Kullback-Leibler (KL) divergence, which regularizes the latent space and encourages the prior to learn expressive, predictive motion patterns.

Trajectory Autoregressive Decoder. The prediction process is initiated by sampling a latent code $\mathbf{z}$ rom the appropriate distribution (the prior p_θ at inference, the posterior q_ϕ at training). This code $\mathbf{z}$, which encapsulates the global motion intent, is concatenated with the last observed state embedding $\mathbf{x}^0$ to form an initial feature vector $\mathbf{f}^0 = \mathbf{x}^0 \oplus \mathbf{Z}$. This initial vector initiates the Trajectory Autoregressive Decoder (TAD) through recurrent updates:

$$\mathbf{f}_t = \mathbf{y}_t \oplus \mathbf{Z}, \quad \mathbf{Z} \sim \begin{cases} q_\phi(\mathbf{Z}|\mathbf{X},\mathbf{Y}) & \textit{(training)} \\ p_\theta(\mathbf{Z}) & \textit{(inference)} \end{cases} \tag{4}$$

where $\mathbf{F}_\mathbf{Y}^t = \{\mathbf{f}^0, ..., \mathbf{f}^t\}$ represents the progressively augmented feature sequence. The decoding mechanism maintains persistent latent guidance by keeping the sampled $\mathbf{Z}$ constant throughout generation, ensuring global motion pattern consistency. Simultaneously, it accumulates dynamic temporal context through the expanding feature sequence $\mathbf{F}_t$, which explicitly preserves historical state dependencies. At each timestep t, the decoder predicts the next trajectory feature $\mathbf{F}_{t+1}$ conditioned on this dual-information representation and then transformed through an MLP to reconstruct the predicted trajectory $\mathbf{y}_{t+1}$. Finally, we get the predicted future trajectory $\hat{\mathbf{Y}}$ of length t_f. The predicted position for the current timestep serves as our final global-aware trajectory proposal, $\mathbf{b}_t^{global}$.

TrajFormer Architecture. Both the encoder and decoder are built upon our TrajFormer block, which adapts the standard Transformer architecture for trajectory modeling. To provide temporal context, we first add a cosine-based positional encoding scheme to the input trajectory coordinates. A TrajFormer block consists of two main sub-layers: multi-head self-attention (MHSA) and a feed-forward network (FFN). For an input sequence $\mathbf{X}_{in}$, the $\mathbf{Q}$, $\mathbf{K}$, $\mathbf{V}$ matrices are first projected:

$$\mathbf{Q} = (\mathbf{X} + \mathrm{PE}(t_p))\mathbf{W}_Q, \tag{5}$$
$$\mathbf{K} = (\mathbf{X} + \mathrm{PE}(t_p))\mathbf{W}_K, \tag{6}$$
$$\mathbf{V} = (\mathbf{X} + \mathrm{PE}(t_p))\mathbf{W}_V \tag{7}$$

The self-attention output is then calculated, followed by residual connections, layer normalization, and an FFN block:

$$\mathbf{X}_{\text{attn}} = \mathrm{Softmax}\left(\frac{\mathbf{Q}\mathbf{K}^\top}{\sqrt{d_k}}\right)\mathbf{V}, \tag{8}$$
$$\mathbf{X}' = \mathrm{LayerNorm}(\mathbf{X}_{in} + \mathbf{X}_{\text{attn}}), \tag{9}$$
$$\mathbf{X}_{\text{out}} = \mathrm{LayerNorm}(\mathbf{X}' + \mathrm{FFN}(\mathbf{X}')) \tag{10}$$

The TrajFormer Decoder block is similar but includes an additional cross-attention layer to incorporate the encoded features from the past trajectory.

Insight and Advantages of IMM. The core insight behind the IMM is the decoupling of long-term motion modeling from the high-bandwidth point cloud data. Unlike sequence-based methods that are burdened by processing multiple, dense point clouds to extract motion cues, our IMM operates on a highly compressed, low-dimensional representation: the historical trajectory of bounding box centers. This design is motivated by the observation that for tracking, the object's macro-level motion continuity (where it's going) is often more critical for overcoming occlusions and sparsity than its micro-level surface details in every historical frame. By learning from the trajectory alone, the IMM can focus exclusively on capturing the object's dynamic behavior over time—such as velocity and turning patterns—creating a robust, global motion prior. This lightweight, information-centric approach is the key to how **TrajTrack** achieves the robustness of a sequence-based method while only introducing a minor computational burden compared to a two-frame tracker.

E. Trajectory-guided Proposal Refinement

The final post-process of TrajTrack is to dynamiclly fuse the proposals from the explicit and implicit motion models. This stage receives two inputs: the agile but potentially noisy local-aware proposal, $\mathbf{b}_t^{\text{local}}$, and the stable, global-aware trajectory proposal, $\mathbf{b}_t^{\text{global}}$. To synergize these two, we introduce a

confidence-based refinement strategy. We use the Intersection-over-Union (IoU) between the two proposals themselves, IoU($\mathbf{b}_t^{\text{local}}$, $\mathbf{b}_t^{\text{global}}$), as a metric for the reliability of the short-term, explicit prediction. **(1)** If the IoU is high (above a threshold λ), it indicates that both short-term and long-term models are in agreement. In this case, we trust the more precise, local-aware proposal, $\mathbf{b}_t^{\text{local}}$, as the final output. **(2)** If the IoU is low, it signals a potential failure of the explicit model, likely due to sparsity or occlusion. In this scenario, we rely on the more stable, long-term trajectory proposal, $\mathbf{b}_t^{\text{global}}$, as a robust fallback. This mechanism allows our tracker to be fast and precise in simple scenarios while leveraging the long-term motion prior to enhance robustness and recover from failures in challenging environments.

F. Loss Function

Our **TrajTrack** framework is trained end-to-end with a composite loss function, $\mathcal{L}_{total}$, which jointly optimizes the explicit motion proposal and the implicit trajectory prediction. **Explicit Motion Loss ($\mathcal{L}_{\text{tracking}}$).** To supervise the initial proposal from Stage 1, we follow [16] and adopt the Residual Log-likelihood Estimation (RLE) loss [44], which reduces the difficulty of regression by adding a hand-designed residual term distribution to the L2 loss term, making the fitted distribution closer to the true distribution, as the tracking loss:

$$\mathcal{L}_{\text{tracking}} = \mathcal{L}_{\text{RLE}}(\mathbf{b}_t^{\text{local}}, \mathbf{b}_t^{gt}) \tag{11}$$

Implicit Trajectory Prediction Loss ($\mathcal{L}_{\text{traj}}$). To train our IMM module from Stage 2, we use the standard negative Evidence Lower Bound (ELBO) loss. This loss comprises a reconstruction term, which ensures the predicted trajectory matches the ground truth, and a KL-divergence term, which regularizes the latent space:

$$\mathcal{L}_{\text{pred}} = \mathcal{L}_{elbo} = -\mathbb{E}_{q_\phi(\mathbf{Z}|\mathbf{Y},\mathbf{X})}[\log p_\theta(\mathbf{Y}|\mathbf{Z},\mathbf{X})] \tag{12}$$

$$+\text{KL}(q_\phi(\mathbf{Z}|\mathbf{Y},\mathbf{X})\|p_\theta(\mathbf{Z}|\mathbf{X})) \tag{13}$$

Overall Objective. The final training objective is a weighted sum of these two losses:

$$\mathcal{L}_{total} = \mathcal{L}_{\text{tracking}} + \lambda \mathcal{L}_{\text{traj}} \tag{14}$$

where λ hyper-parameter that balances the contribution of the trajectory prediction task.

IV. Experiments

Dataset and Metrics. We follow the common setup [9], [49] and conduct experiments on the large-scale nuScenes [50] dataset. Notably, due to the limited data size of the KITTI dataset (only 19 training, 2 validation sequences [7], [46]) makes it challenging to adequately evaluate the methods. In contrast, the nuScenes dataset comprises 700 training and 150 validation sequences, across 40K point cloud frames, allowing for a more comprehensive evaluation. The evaluation metrics is followed the common setup [3], [6], [7] to report *Success* and *Precision* based on one pass evaluation (OPE) [51], [52].
Implementation Details. We follow previous works [3], [7], [16], set the previous frame $t-1$ is set as the template and the current frame t as the search region. These cropped regions, defined as $[(-4.8,4.8),(-4.8,4.8),(-1.5,1.5)]$ for cars and $[(-1.92,1.92),(-1.92,1.92),(-1.5,1.5)]$ for humans along the (x,y,z) axes. Additionally, the data augmentation, such as random horizontal flipping and uniform rotation within [-5°,5°] is applied to target points and bounding boxes to improve the model's generalization. All experiments are conducted on NVIDIA RTX 3090 GPUs. The network is trained for 20 epochs with the AdamW optimizer, initialized with a learning rate of 0.0001, with a batch size is 32. Our experiment video is available at https://www.bilibili.com/video/BV1ahYgzmEWP.

A. Comparison on nuScenes dataset:

To rigorously evaluate our framework under challenging real-world conditions, we conduct comprehensive comparisons on the challenging nuScenes dataset, characterized by complex scenes and sparser point clouds from 32-beam LiDARs data in diverse scenes. As shown in Tab. I, our TrajTrack consistently outperforms all prior trackers across all categories, demonstrating its exceptional scalability and robustness in sparse and diverse environments. For instance, TrajTrack it surpasses a strong baseline, P2P [16], by in the Car and Pedestrian category by 4.13/3.82% in Success/Precision for the Car category and by an even more significant 4.55/6.81% for the Pedestrian category. This robust performance in a sparse environment highlights the core advantage of our trajectory-based paradigm: by leveraging lightweight, long-term motion continuity, our method maintains a stable track where methods relying solely on instantaneous cues falter.
Running Speed: Inference speed is also a vital factor for practical applications. We present a comprehensive speed comparison of TrajTrack with other methods in Tab. II. Following common evaluation protocols [3], [6], [16], speed is measured by calculating the average running time of all frames in the Car category. On a single NVIDIA RTX 3090 GPU, TrajTrack achieves 56.3 FPS. Despite the computational overhead incurred by our IMM module, TrajTrack yields significant performance improvements, maintaining a better trade-off between accuracy and speed.
Generalizability Across Different Trackers: To demonstrate the versatility of our trajectory-based paradigm, we replaced two distinct baselines into our framework with Implicit Motion Modeling (IMM) module. As illustrated in the Tab. III, when applied our method to the similarity-based paradigm BAT [5] and the motion-based paradigm M^2-Track [9], consistently and significantly achieving improvements of 2.31/3.14% and 6.34/8.37% in Success/Precision, respectively.This demonstrates that our approach of leveraging long-term motion continuity is a general principle that can enhance various 3D SOT architectures, regardless of their underlying paradigm.
Robustness to Sparsity: We evaluated our method's performance under varying levels of point cloud sparsity by analyzing its accuracy based on the number of points in the initial template. As shown in Fig. 4, TrajTrack consistently outperforms other leading methods, especially in extremely sparse scenarios. On the nuScenes dataset, where a majority of tracklets begin with fewer than 15 points, our method's advantage is most pronounced. This highlights its superior ability

TABLE I: Comparison with SOTA methods on the NuScenes dataset. Success and Precision are used for evaluation, **Bold** and underline denote the best result and the second-best one, respectively.

Method	Publish	Paradigm	Car [64,159]	Pedestrian [33,227]	Truck [13,587]	Trailer [3,352]	Bus [2,953]	Mean [117,278]
SC3D [1]	CVPR'19	Two-frame	22.31 / 21.93	11.29 / 12.65	35.28 / 28.12	35.28 / 28.12	29.35 / 24.08	20.70 / 20.20
P2B [3]	CVPR'20		38.81 / 43.81	28.39 / 52.24	48.96 / 40.05	48.96 / 40.05	32.95 / 27.41	36.48 / 45.08
PTT [7]	IROS'21		41.22 / 45.26	19.33 / 32.03	50.23 / 48.56	51.70 / 46.50	39.40 / 36.70	36.33 / 41.72
BAT [5]	ICCV'21		40.73 / 43.29	28.83 / 53.32	52.59 / 44.89	52.59 / 44.89	35.44 / 28.01	38.10 / 45.71
V2B [29]	NIPS'21		54.40 / 59.70	30.10 / 55.40	53.70 / 54.50	54.90 / 51.44	- / -	- / -
M^2-Track [9]	CVPR'22		55.85 / 65.09	32.10 / 60.92	57.36 / 59.54	57.61 / 58.26	51.39 / 51.44	49.23 / 62.73
PTTR [8]	CVPR'22		51.89 / 58.61	29.90 / 45.09	45.30 / 44.74	45.87 / 38.36	43.14 / 37.74	44.50 / 52.07
SMAT [45]	RAL'22		43.51 / 49.04	32.27 / 60.28	- / -	- / -	39.42 / 34.32	- / -
GLT-T [46]	AAAI'23		48.52 / 54.29	31.74 / 56.49	52.74 / 51.43	57.60 / 52.01	44.55 / 40.69	44.42 / 54.33
MLSET [47]	RAL'23		53.20 / 58.30	33.20 / 58.60	54.30 / 52.50	53.10 / 40.90	- / -	- / -
PTTR++ [48]	PAMI'24		59.96 / 66.73	32.49 / 50.50	59.85 / 61.20	54.51 / 50.28	53.98 / 51.22	51.86 / 60.63
FlowTrack [12]	IROS'24		60.29 / 71.07	37.60 / 67.64	- / -	55.39 / 62.70	- / -	- / -
P2P [16]	IJCV'25		65.15 / 72.90	46.43 / 75.08	64.96 / 65.96	70.46 / 66.86	59.02 / 56.56	59.84 / 72.13
STTracker [17]	RAL'23	Sequence	56.11 / 69.07	37.58 / 68.36	54.29 / 60.71	48.13 / 55.40	36.31 / 36.07	49.66 / 66.77
SeqTrack3D [18]	ICRA'24		62.55 / 71.46	39.94 / 68.57	60.97 / 63.04	68.37 / 61.76	54.33 / 53.52	55.92 / 68.94
TrajTrack	Ours	Trajectory	**69.28 / 76.72**	**50.98 / 81.89**	**68.19 / 69.44**	**70.70 / 68.02**	**61.16 / 57.67**	**63.81 / 76.61**
Improvement			↑ 4.13 / ↑ 3.82	↑ 4.55 / ↑ 6.81	↑ 3.23 / ↑ 3.48	↑ 0.24 / ↑ 1.16	↑ 2.14 / ↑ 1.11	↑ 3.97 / ↑ 4.48

TABLE II: Comparison of the running speeds on different representative methods.

Method	P2B [3]	PTT [7]	BAT [5]	LTTR [31]
FPS	40.0	40.0	57.0	23.0
Method	M^2Track [9]	GLT-T [46]	PTTR++ [48]	M^2Track++ [10]
FPS	51.2	30.0	43.0	57.0
Method	STTracker [17]	SeqTrack3D [18]	P2P [16]	**TrajTrack (Ours)**
FPS	22.0	38.0	63.9	**56.3**

TABLE III: Ablation Study on Different Baselines

Method	**M^2-Track** [9]	**BAT** [5]
Baseline	55.85 / 65.09	40.73 / 43.29
w/ TrajTrack	58.16 / 68.23	47.07 / 51.66
improvement	↑ **2.31 / 3.14**	↑ **6.34 / 8.37**

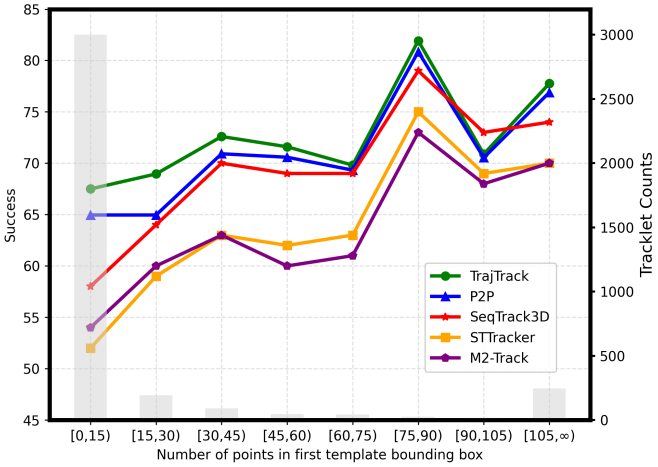

Fig. 4: Tracking performance across varying numbers of template points in the first frame.

to leverage long-term motion continuity when instantaneous appearance cues are minimal. To further validate this, we identified a challenging subset where over half the frames contain fewer than 20 points. On these 3,061 tracklets, our method achieves a Success/Precision of 67.28% / 75.69%, significantly outperforming the baseline's 65.16% / 72.57%, which confirms its enhanced robustness in low-density conditions.

B. Ablation Study

TABLE IV: Ablation Study of components in TrajTrack.

IMM Setting	**Car**		**Ped**	
	Succ.	Prec.	Succ.	Prec.
Baseline [16]	65.15	72.90	46.43	75.08
MLP-based IMM	67.77	75.67	51.00	81.64
TrajFormer-based IMM	**69.28**	**76.72**	**51.01**	**81.89**

We analyze the core Implicit Motion Modeling module of our method in Tab. IV. Compared to the baseline tracker [16], which relies solely on explicit two-frame motion, incorporating a simple MLP-based IMM already yields substantial performance gains, especially for the Pedestrian category (+4.61% Success). This result validates the core premise of our work: leveraging implicit motion continuity from past trajectories is highly effective. By further employing our more powerful TrajFormer-based IMM, the performance is enhanced to its peak. This systematically demonstrates that while the IMM concept itself is beneficial, the TrajFormer architecture is key to fully capturing the complex temporal dependencies in the trajectory data.

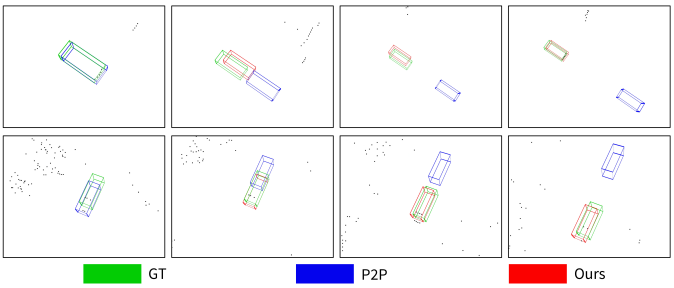

Fig. 5: **Visualization results on sparse point cloud scenes.**

C. Visualization results.

To provide a qualitative evaluation, we visualize our tracking results against a strong baseline [16] in various challenging scenes. As shown in Fig. 6, our TrajTrack consistently demonstrates more accurate and stable tracking than the baseline. When the baseline tracker begins to fail due to occlusion or

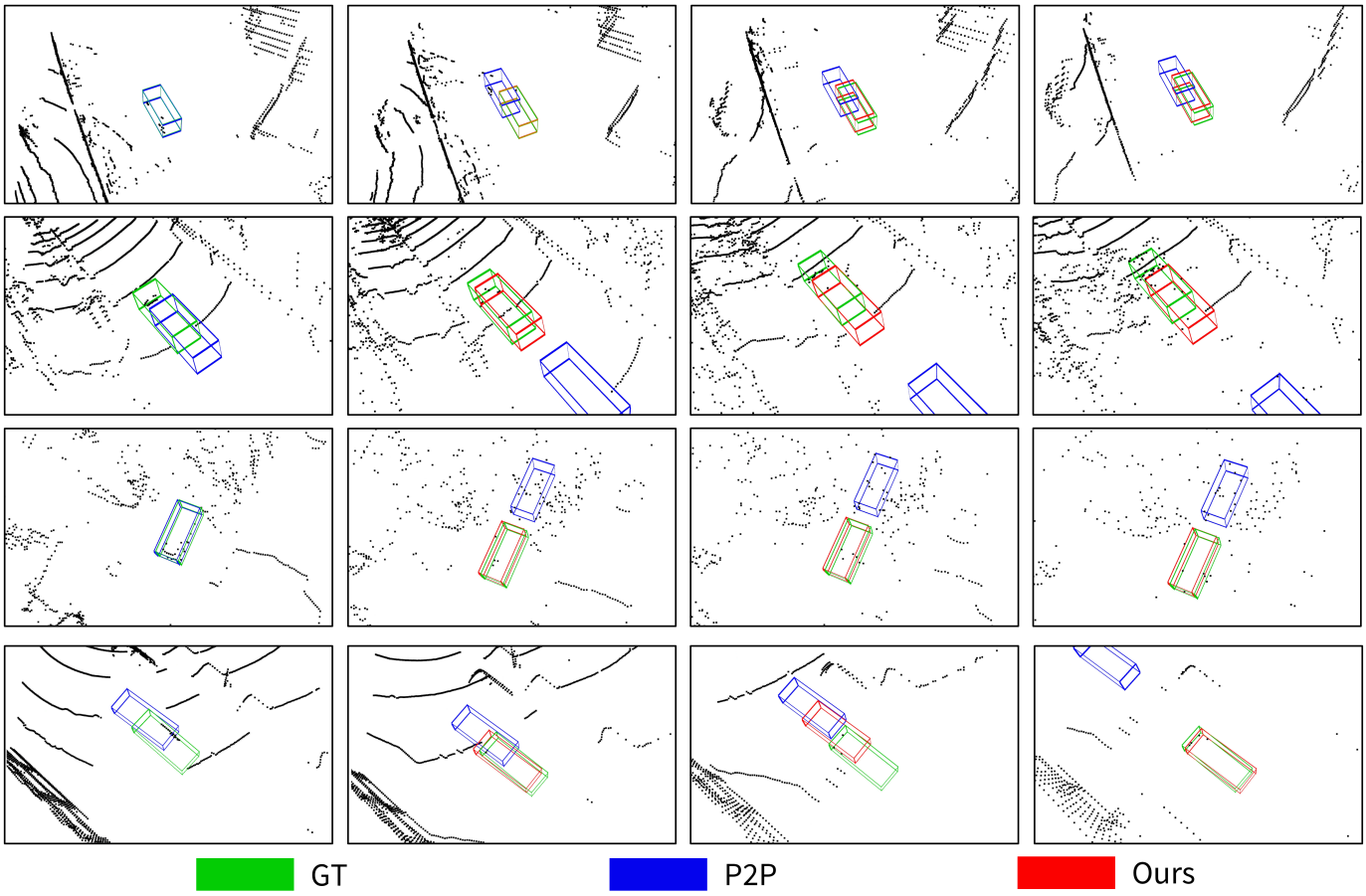

Fig. 6: **Visualization results on NuScenes.** Starting from the second frame, the global-aware trajectory proposal from Implicit Motion Modeling corrects the biased tracking results, achieving accurate tracking.

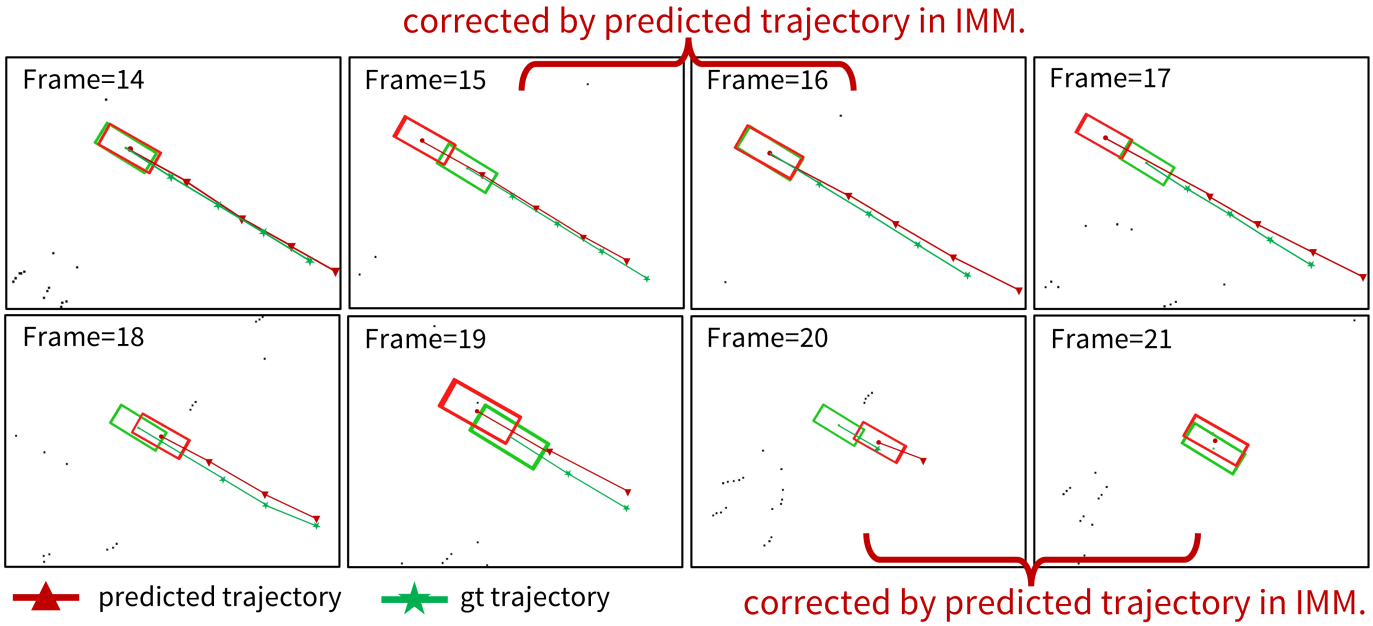

Fig. 7: **Visualization results with Implicit Trajectory Prediction correction.**

sparsity, our Trajectory-guided Proposal Refinement mechanism integrates a global-aware trajectory proposal from the Implicit Motion Modeling. This allows our method to leverage the long-term motion prior to correct misaligned bounding boxes and effectively recover the track, preventing the failure from error accumulation.Additionally, as illustrated in Fig. 7, while tracking failed, the subsequent prediction can still be corrected by leveraging long-term motion information. Furthermore, Fig. 5 highlights our method's robustness in extremely sparse scenes. Even when the target is represented by only a few scattered points, TrajTrack successfully leverages temporal consistency to track accurately. These visualizations

confirm that the synergistic integration of short-term motion and long-term trajectory priors significantly enhances tracking reliability in dynamic and complex scenes.

V. CONCLUSIONS

In this work, we introduced **TrajTrack**, a novel trajectory-based paradigm for 3D single object tracking that resolves the critical trade-off between the robustness of two-frame methods and the efficiency of sequence-based approaches. Our key innovation is an Implicit Motion Modeling (IMM) module that leverages lightweight, historical bounding box trajectories to learn long-term motion continuity. By synergistically refining a short-term, explicit motion proposal with this powerful long-term prior, TrajTrack achieves a new state-of-the-art tracking performance in the challenging nuScenes dataset, while maintaining real-time speed. For future work, we plan to explore tighter fusion strategies between the explicit and implicit modules and investigate the application of this lightweight temporal modeling approach to other robotics perception tasks.

VI. LIMITATION AND FUTURE WORK

Despite its strong performance, TrajTrack has several limitations. First, our current Trajectory-guided proposal refinement is a heuristic; a more deeply integrated, learnable fusion mechanism might yield further improvements. Second, the model currently relies only on geometric information. Scenarios with fewer appearance or color features could lead to identity switches during long-term tracking. Third, model latency still needs to improve for on-board application. One promising direction is to use the quantization technique [53], [54] to compress the model and accelerate the inference speed. Beyond trajectory aggregation, we can include the fusion of multi-modal sensor data [49], such as incorporating dense image information alongside LiDAR point clouds. Besides, while our current focus is on LiDAR's intrinsic geometric cues, advancements in image understanding and generation [55]–[57], like diffusion models for cross-domain image composition, demonstrate the powerful capabilities of modern image processing. Future work can investigate how these advanced image features, enriched by generative priors and semantic controls, might contribute to more robust and context-aware 3D tracking, particularly in challenging, sparse conditions.

REFERENCES

[1] S. Giancola, J. Zarzar, and B. Ghanem, "Leveraging shape completion for 3d siamese tracking," in *Proceedings of the IEEE/CVF conference on computer vision and pattern recognition*, pp. 1359–1368, 2019.

[2] Y. Cui, Z. Fang, and S. Zhou, "Point siamese network for person tracking using 3d point clouds," *Sensors*, vol. 20, no. 1, p. 143, 2019.

[3] H. Qi, C. Feng, Z. Cao, F. Zhao, and Y. Xiao, "P2b: Point-to-box network for 3d object tracking in point clouds," in *Proceedings of the IEEE/CVF conference on computer vision and pattern recognition*, pp. 6329–6338, 2020.

[4] Z. Fang, S. Zhou, Y. Cui, and S. Scherer, "3d-siamrpn: An end-to-end learning method for real-time 3d single object tracking using raw point cloud," *IEEE Sensors Journal*, vol. 21, no. 4, pp. 4995–5011, 2020.

[5] C. Zheng, X. Yan, J. Gao, W. Zhao, W. Zhang, Z. Li, and S. Cui, "Box-aware feature enhancement for single object tracking on point clouds," in *International Conference on Computer Vision*, pp. 13199–13208, 2021.

[6] J. Shan, S. Zhou, Z. Fang, and Y. Cui, "Ptt: Point-track-transformer module for 3d single object tracking in point clouds," in *2021 IEEE/RSJ International Conference on Intelligent Robots and Systems (IROS)*, pp. 1310–1316, IEEE, 2021.

[7] S. Jiayao, S. Zhou, Y. Cui, and Z. Fang, "Real-time 3d single object tracking with transformer," *IEEE Transactions on Multimedia*, pp. 1–1, 2022.

[8] C. Zhou, Z. Luo, Y. Luo, T. Liu, L. Pan, Z. Cai, H. Zhao, and S. Lu, "Pttr: Relational 3d point cloud object tracking with transformer," in *Computer Vision and Pattern Recognition*, pp. 8531–8540, 2022.

[9] C. Zheng, X. Yan, H. Zhang, B. Wang, S. Cheng, S. Cui, and Z. Li, "Beyond 3d siamese tracking: A motion-centric paradigm for 3d single object tracking in point clouds," in *Proceedings of the IEEE/CVF Conference on Computer Vision and Pattern Recognition*, pp. 8111–8120, 2022.

[10] C. Zheng, X. Yan, H. Zhang, B. Wang, S. Cheng, S. Cui, and Z. Li, "An effective motion-centric paradigm for 3d single object tracking in point clouds," *IEEE Transactions on Pattern Analysis and Machine Intelligence*, 2023.

[11] Y. Xia, Q. Wu, W. Li, A. B. Chan, and U. Stilla, "A lightweight and detector-free 3d single object tracker on point clouds," *IEEE Transactions on Intelligent Transportation Systems*, 2023.

[12] S. Li, Y. Cui, Z. Li, and Z. Fang, "Flowtrack: Point-level flow network for 3d single object tracking," *2024 IEEE/RSJ International Conference on Intelligent Robots and Systems (IROS)*, 2024.

[13] Y. Lu, J. Nie, Z. He, H. Gu, and X. Lv, "Voxeltrack: Exploring multi-level voxel representation for 3d point cloud object tracking," in *Proceedings of the 32nd ACM International Conference on Multimedia*, pp. 6345–6354, 2024.

[14] W. Xu, S. Zhou, and Z. Yuan, "Pillartrack: Redesigning pillar-based transformer network for single object tracking on point clouds," *arXiv preprint arXiv:2404.07495*, 2024.

[15] S. Zhou, N. Jiahao, Z. Ziyu, C. Yichao, and L. Xiaobo, "Focustrack: One-stage focus-and-suppress framework for 3d point cloud object tracking," in *Proceedings of the 33rd ACM International Conference on Multimedia*, 2025.

[16] J. Nie, F. Xie, S. Zhou, X. Zhou, D.-K. Chae, and Z. He, "P2p: Part-to-part motion cues guide a strong tracking framework for lidar point clouds," *arXiv preprint arXiv:2407.05238v2*, vol. abs/2407.05238, 2024.

[17] Y. Cui, Z. Li, and Z. Fang, "Sttracker: Spatio-temporal tracker for 3d single object tracking," *IEEE Robotics and Automation Letters*, vol. 8, no. 8, pp. 4967–4974, 2023.

[18] Y. Lin, Z. Li, Y. Cui, and Z. Fang, "Seqtrack3d: Exploring sequence information for robust 3d point cloud tracking," in *2024 IEEE International Conference on Robotics and Automation (ICRA)*, pp. 6959–6965, 2024.

[19] S. Zhou, Z. Yuan, D. Yang, X. Hu, J. Qian, and Z. Zhao, "Pillarhist: A quantization-aware pillar feature encoder based on height-aware histogram," in *Proceedings of the Computer Vision and Pattern Recognition Conference*, pp. 27336–27345, 2025.

[20] S. Zhou, Z. Tian, X. Chu, X. Zhang, B. Zhang, X. Lu, C. Feng, Z. Jie, P. Y. Chiang, and L. Ma, "Fastpillars: A deployment-friendly pillar-based 3d detector," *arXiv preprint arXiv:2302.02367*, 2023.

[21] J. Liu, G. Wang, Z. Liu, C. Jiang, M. Pollefeys, and H. Wang, "Regformer: an efficient projection-aware transformer network for large-scale point cloud registration," in *Proceedings of the IEEE/CVF International Conference on Computer Vision*, pp. 8451–8460, 2023.

[22] J. Liu, R. Yu, Y. Wang, Y. Zheng, T. Deng, W. Ye, and H. Wang, "Point mamba: A novel point cloud backbone based on state space model with octree-based ordering strategy," *arXiv preprint arXiv:2403.06467*, 2024.

[23] J. Liu, J. Han, L. Liu, A. I. Aviles-Rivero, C. Jiang, Z. Liu, and H. Wang, "Mamba4d: Efficient 4d point cloud video understanding with disentangled spatial-temporal state space models," in *Proceedings of the Computer Vision and Pattern Recognition Conference*, pp. 17626–17636, 2025.

[24] S. Zhou, Z. Yuan, D. Yang, Z. Zhao, X. Hu, Y. Shi, X. Lu, and Q. Wu, "Information entropy guided height-aware histogram for quantization-friendly pillar feature encoder," *arXiv preprint arXiv:2405.18734*, 2024.

[25] Y. Zheng, B. Zhong, Q. Liang, Z. Mo, S. Zhang, and X. Li, "Odtrack: Online dense temporal token learning for visual tracking," in *Proceedings of the AAAI conference on artificial intelligence*, vol. 38, pp. 7588–7596, 2024.

[26] Y. Zheng, B. Zhong, Q. Liang, Z. Tang, R. Ji, and X. Li, "Leveraging local and global cues for visual tracking via parallel interaction network," *IEEE Transactions on Circuits and Systems for Video Technology*, vol. 33, no. 4, pp. 1671–1683, 2022.

[27] Y. Zheng, B. Zhong, Q. Liang, G. Li, R. Ji, and X. Li, "Toward unified token learning for vision-language tracking," *IEEE Transactions on Circuits and Systems for Video Technology*, vol. 34, no. 4, pp. 2125–2135, 2023.

[28] C. R. Qi, O. Litany, K. He, and L. J. Guibas, "Deep hough voting for 3d object detection in point clouds," in *ICCV*, pp. 9277–9286, 2019.

[29] L. Hui, L. Wang, M. Cheng, J. Xie, and J. Yang, "3d siamese voxel-to-bev tracker for sparse point clouds," *Advances in Neural Information Processing Systems*, vol. 34, pp. 28714–28727, 2021.

[30] L. Hui, L. Wang, L. Tang, K. Lan, J. Xie, and J. Yang, "3d siamese transformer network for single object tracking on point clouds," in *ECCV*, 2022.

[31] Y. Cui, Z. Fang, J. Shan, Z. Gu, and S. Zhou, "3d object tracking with transformer," in *The British Machine Vision Conference*, 2021.

[32] K. Lan, H. Jiang, and J. Xie, "Temporal-aware siamese tracker: Integrate temporal context for 3d object tracking," in *Proceedings of the Asian Conference on Computer Vision*, pp. 399–414, 2022.

[33] J. Gao, C. Sun, H. Zhao, Y. Shen, D. Anguelov, C. Li, and C. Schmid, "Vectornet: Encoding hd maps and agent dynamics from vectorized representation," in *2020 IEEE/CVF Conference on Computer Vision and Pattern Recognition (CVPR)*, pp. 11522–11530, 2020.

[34] W. Zeng, M. Liang, R. Liao, and R. Urtasun, "Lanercnn: Distributed representations for graph-centric motion forecasting," in *2021 IEEE/RSJ International Conference on Intelligent Robots and Systems (IROS)*, pp. 532–539, 2021.

[35] H. Cheng, M. Liu, L. Chen, H. Broszio, M. Sester, and M. Y. Yang, "Gatraj: A graph-and attention-based multi-agent trajectory prediction model," *ISPRS Journal of Photogrammetry and Remote Sensing*, vol. 205, pp. 163–175, 2023.

[36] H. Zhao, J. Gao, T. Lan, C. Sun, B. Sapp, B. Varadarajan, Y. Shen, Y. Shen, Y. Chai, C. Schmid, *et al.*, "Tnt: Target-driven trajectory prediction," in *Conference on Robot Learning. PMLR, 2021*, pp. 895–904, 2021.

[37] J. Gu, C. Sun, and H. Zhao, "Densetnt: End-to-end trajectory prediction from dense goal sets," in *Proceedings of the IEEE/CVF International Conference on Computer Vision*, pp. 15303–15312, 2021.

[38] W. Wu, X. Feng, Z. Gao, and Y. Kan, "Smart: Scalable multi-agent real-time simulation via next-token prediction," *arXiv preprint arXiv:2405.15677*, 2024.

[39] B. Ivanovic and M. Pavone, "The trajectron: Probabilistic multi-agent trajectory modeling with dynamic spatiotemporal graphs," in *2019 IEEE/CVF International Conference on Computer Vision (ICCV)*, pp. 2375–2384, 2019.

[40] A. Gupta, J. Johnson, L. Fei-Fei, S. Savarese, and A. Alahi, "Social gan: Socially acceptable trajectories with generative adversarial networks," in *IEEE Conference on Computer Vision and Pattern Recognition (CVPR)*, no. CONF, 2018.

[41] W. Chen, F. Wang, and H. Sun, "S2tnet: Spatio-temporal transformer networks for trajectory prediction in autonomous driving," in *Proceedings of The 13th Asian Conference on Machine Learning*, vol. 157, pp. 454–469, 17–19 Nov 2021.

[42] Y. Yuan, X. Weng, Y. Ou, and K. Kitani, "Agentformer: Agent-aware transformers for socio-temporal multi-agent forecasting," in *Proceedings of the IEEE/CVF International Conference on Computer Vision (ICCV)*, 2021.

[43] H. Yadav, M. Schaefer, K. Zhao, and T. Meisen, "Caspformer: Trajectory prediction from bev images with deformable attention," in *Pattern Recognition* (A. Antonacopoulos, S. Chaudhuri, R. Chellappa, C.-L. Liu, S. Bhattacharya, and U. Pal, eds.), (Cham), pp. 420–434, Springer Nature Switzerland, 2025.

[44] J. Li, S. Bian, A. Zeng, C. Wang, B. Pang, W. Liu, and C. Lu, "Human pose regression with residual log-likelihood estimation," in *2021 IEEE/CVF International Conference on Computer Vision (ICCV)*, pp. 11005–11014, 2021.

[45] Y. Cui, J. Shan, Z. Gu, Z. Li, and Z. Fang, "Exploiting more information in sparse point cloud for 3d single object tracking," *IEEE Robotics and Automation Letters*, vol. 7, no. 4, pp. 11926–11933, 2022.

[46] J. Nie, Z. He, Y. Yang, M. Gao, and J. Zhang, "Glt-t: Global-local transformer voting for 3d single object tracking in point clouds," in *Proceedings of the AAAI Conference on Artificial Intelligence*, vol. 37, pp. 1957–1965, 2023.

[47] Q. Wu, C. Sun, and J. Wang, "Multi-level structure-enhanced network for 3d single object tracking in sparse point clouds," *IEEE Robotics and Automation Letters*, vol. 8, no. 1, pp. 9–16, 2023.

[48] Z. Luo, C. Zhou, L. Pan, G. Zhang, T. Liu, Y. Luo, H. Zhao, Z. Liu, and S. Lu, "Exploring point-bev fusion for 3d point cloud object tracking with transformer," *IEEE transactions on pattern analysis and machine intelligence*, 2024.

[49] Z. Hu, S. Zhou, S. Zhao, and Z. Yuan, "Mvctrack: Boosting 3d point cloud tracking via multimodal-guided virtual cues," 2024.

[50] H. Caesar, V. Bankiti, A. H. Lang, S. Vora, V. E. Liong, Q. Xu, A. Krishnan, Y. Pan, G. Baldan, and O. Beijbom, "nuscenes: A multimodal dataset for autonomous driving," in *Proceedings of the IEEE/CVF conference on computer vision and pattern recognition*, pp. 11621–11631, 2020.

[51] Y. Wu, J. Lim, and M.-H. Yang, "Online object tracking: A benchmark," in *Proceedings of the IEEE conference on computer vision and pattern recognition*, pp. 2411–2418, 2013.

[52] M. Kristan, J. Matas, A. Leonardis, T. Vojíř, R. Pflugfelder, G. Fernandez, G. Nebehay, F. Porikli, and L. Čehovin, "A novel performance evaluation methodology for single-target trackers," *IEEE transactions on pattern analysis and machine intelligence*, vol. 38, no. 11, pp. 2137–2155, 2016.

[53] S. Zhou, L. Li, X. Zhang, B. Zhang, S. Bai, M. Sun, Z. Zhao, X. Lu, and X. Chu, "Lidar-ptq: Post-training quantization for point cloud 3d object detection," *International Conference on Learning Representations (ICLR)*, 2024.

[54] J. Yu, C. Shu, D. Yang, S. Zhou, Z. Yu, X. Hu, and Y. Chen, "Q-petr: Quant-aware position embedding transformation for multi-view 3d object detection," 2025.

[55] S. Lu, Y. Liu, and A. W.-K. Kong, "Tf-icon: Diffusion-based training-free cross-domain image composition," in *Proceedings of the IEEE/CVF International Conference on Computer Vision*, pp. 2294–2305, 2023.

[56] S. Lu, Z. Wang, L. Li, Y. Liu, and A. W.-K. Kong, "Mace: Mass concept erasure in diffusion models," in *Proceedings of the IEEE/CVF Conference on Computer Vision and Pattern Recognition*, pp. 6430–6440, 2024.

[57] S. Lu, Z. Zhou, J. Lu, Y. Zhu, and A. W.-K. Kong, "Robust watermarking using generative priors against image editing: From benchmarking to advances," *arXiv preprint arXiv:2410.18775*, 2024.